12th International Symposium on Turbulence and Shear Flow Phenomena (TSFP12)
Osaka, Japan (Online), July 19-22, 2022

WALL-MODELLED LES USING HIGH- AND LOW-ORDER CFD CODES: APPLICATION TO A FLAT-PLATE BOUNDARY LAYER

Timofey Mukha
SimEx/FLOW, Engineering Mechanics
KTH Royal Institute of Technology
SE-100 44 Stockholm, Sweden
tmu@kth.se

Philipp Schlatter
SimEx/FLOW, Engineering Mechanics
KTH Royal Institute of Technology
SE-100 44 Stockholm, Sweden
pschlatt@mech.kth.se

ABSTRACT

Results from wall-modelled large-eddy simulations of a zero-pressure-gradient flat-plate turbulent boundary layer in the range $Re_\theta \approx [4000, 12000]$ are reported. The simulations are performed using a low- and a high-order code: OpenFOAM® and Nek5000, respectively. For the latter, such simulations have previously not been reported in the literature. Structured hexahedral meshes are used, with two levels of refinement. As an important aspect in the wall modelling methodology, we use a temporally varying wall viscosity in order to enforce the wall shear stress. An equivalent inflow generation procedure is used for both codes, allowing for a more fair comparison. Results from Nek5000 simulations are generally more accurate. Both the skin friction and the profiles of velocity statistics are in good agreement with reference data. For Nek5000, this is an important milestone in the development of wall modelling capabilities for this solver. The results from OpenFOAM simulations exhibit a significant over-prediction of the skin friction, which has not been previously reported in the literature. Further investigation of the simulation methodology is necessary to find the cause of the problematic behaviour.

INTRODUCTION

In the context of large-eddy simulation (LES) wall modelling typically refers to introducing additional equations that couple the flow quantities in the boundary layer's outer region with the value of the wall-shear stress. In principle, this allows to leave the inner region of the turbulent boundary layer (TBL) unresolved by the grid, leading to more favourable scaling of the grid size with the Reynolds number of the flow. While, in spite of these savings, wall-modelled LES (WMLES) remains computationally expensive, a surge of interest in WMLES could be observed in the recent years, with many new contributions to the literature. For a review of the topic the reader is referred to (Bose & Park, 2018; Larsson *et al.*, 2016).

In this work, we present results from WMLES of a flat-plate turbulent boundary layer. The focus is on comparing the predictive accuracy of two solvers: OpenFOAM and Nek5000. These software vary greatly in the numerical approach to solving the LES equations, OpenFOAM being based on finite volume discretization and Nek5000 on the spectral element method. The latter has the advantage of being high order, whereas using finite volumes offers the benefit of generality with respect to the shape of the computational grid cells.

In OpenFOAM, wall modelling for LES has been previously developed in Mukha *et al.* (2019). But for Nek5000 the development is ongoing, and we are the first to demonstrate the application of WMLES to a developing boundary layer using this solver. The presented comparison allows to highlight both the advantages and the difficulties of conducting WMLES in a high-order code.

SIMULATION SETUP

A summary of the simulation parameters is provided in Table 1. The computational domain is a box of size $150\delta_{99}^i \times 20\delta_{99}^i \times 20\delta_{99}^i$, where δ_{99}^i is the thickness of the inflow boundary layer. The applied boundary conditions are as follows. The Synthetic Eddy Method (SEM) (Jarrin *et al.*, 2006; Poletto *et al.*, 2013) is used to generate the inflow turbulence, corresponding to a flat-plate boundary layer at $Re_\theta \approx 4000$. The profiles of the mean velocity, turbulent kinetic energy and turbulent length scale necessary for the SEM are obtained from the DNS of Schlatter & Örlü (2010). To avoid introducing velocity fluctuations that are too large, we found it necessary to avoid generating the synthetic eddies at $y^+ \lessapprox 20$, where y is the wall-normal coordinate. This location is below the first off-wall grid node, which is located at $y^+ \approx 37$ on the finest grid. The inflow generator is adopted from Hufnagel *et al.* (2018), with the implementation available in Nek5000. For the OpenFOAM simulations, a dummy Nek5000 simulation with a just few elements in the streamwise direction was used. In this simulation, velocity signals were probed at all the locations of the OpenFOAM inflow meshes for $y < 3\delta_{99}^i$. This data was then converted to an appropriate format for OpenFOAM to read from disk. As a result, both solvers use exactly the same inflow generation procedure.

At the top boundary a mixed boundary condition is used, assigning the streamwise velocity to the freestream value U_0, the lateral velocity to 0, and using a homogeneous Neumann condition for the vertical velocity.

At the outflow, a homogeneous Neumann condition for the velocity is used and a homogeneous Dirichlet condition for the pressure.

At the wall, the boundary condition is determined by the wall model. Since wall modelling is the primary concern of this work, it is discussed separately in more detail in the following section.

Unfortunately, the subgrid-scale (SGS) models available for selection in both codes are not the same. For this reason, in OpenFOAM, the WALE model (Nicoud & Ducros, 1999) is used, whereas in Nek5000 the Vreman (2004) model is employed. However, both models are algebraic and therefore similar in terms of computational complexity. In the case of OpenFOAM, WALE has been shown to be a good choice for WMLES in previous works Rezaeiravesh *et al.* (2019). Conversely, for Nek5000 the model selection is still actively researched. Preliminary results from channel flow simulations using the Vreman model have shown good agreement with reference data.

For OpenFOAM, the selection of the scheme for interpolating the convective fluxes is important. Here, a scheme linearly blending linear interpolation with second-order upwind interpolation is used. The weight of the linear scheme is 0.75. This scheme is second-order accurate but quite diffusive due to the upwinding. It would be possible to use linear interpolation only, however the blended scheme is known to keep simulations stable even for highly unstructured grids. The OpenFOAM setup is thus representative of what one would use in an industrial flow simulation. For time-integration, a second-order backward-differencing scheme is used.

In Nek5000, the most important choice is the order of the interpolating polynomials. Here, we use order 7, which is a well-tested selection. This refers to the basis used for the velocity field. For pressure, the polynomials are lower by two orders as part of the pressure-velocity coupling approach referred to as $\mathbb{P}_N$-$\mathbb{P}_{N-2}$, which allows to avoid spurious modes in the pressure field (see Deville *et al.* (2012) for details). Different time-integration schemes are applied to different terms of the momentum equation. For the viscous term, a third-order backward-differencing scheme is used, whereas third-order extrapolation is applied to the convective and source terms, see Karniadakis *et al.* (1991).

Finally, in both codes adaptive time-stepping was used to maintain a CFL number of ≈ 0.5. Time-averaging was performed over $700\delta_{99}^i/U_0$, which is equivalent to about 27 eddy turnover times.

Two meshes were employed for each code, referred to as M1 and M2. In the region occupied by the boundary layer, the meshes are isotropic, and the resolution is defined by the number of Nek5000 elements covering δ_{99}^i: 1 and 2 for M1 and M2, respectively. The same resolution is maintained up to $y = 4\delta_{99}^i$ after which the grid is coarsened in the wall-normal direction. In OpenFOAM, the corresponding grids are constructed considering that each Nek5000 element contains 7 intervals along a single edge. Therefore, 7 and 14 cells cover δ_{99}^i in the two OpenFOAM grids. Additionally, we make use of the fact that OpenFOAM supports unstructured grids by coarsening the grid in the wall-parallel direction at $y = 4\delta_{99}^i$ for the denser grid. An illustration of the M2 grid for both codes is given in Figure 1. It should be noted that even the M2 grid is coarse as one would ideally want to resolve δ_{99}^i by at least 4 elements (or 28 cells with OpenFOAM) across the whole range of Re_θ. However, the corresponding grid size becomes prohibitively large. In the region occupied by the TBL ($y < 4\delta_{99}^i$) the M1 and M2 meshes have, respectively, $\approx 4 \cdot 10^6$ and $\approx 32 \cdot 10^6$ degrees of freedom (DOFs). The latter refers to the number of cells for OpenFOAM and number of nodes for Nek5000.

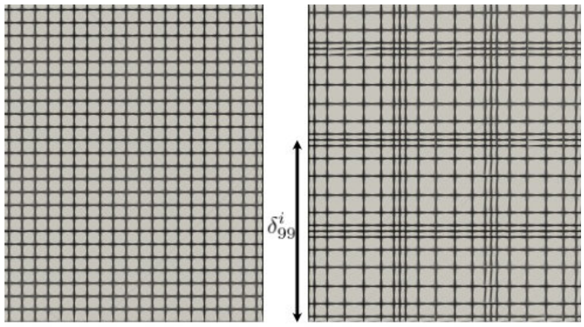

Figure 1. A portion of the computational mesh M2 at the inlet of the domain OpenFOAM (left) and Nek5000 (right).

While the resolution of the outer scales is defined by the grid construction strategy, the resolution in wall units is an outcome of the simulation. This result is shown in Figure 2. The top plot shows the distribution of y_1^+. Clearly, all meshes are very coarse by this measure. Since $\Delta x^+ = \Delta z^+$ it suffices to consider one of these quantities. The bottom plot in Figure 2 shows Δx^+, and to make the plot clear only a small range in x is depicted. The modulation of the values by the change in the inner length scale can be inferred from the behaviour of y_1^+. One clearly sees the large effect of the predefined distribution of nodes within the element in Nek5000. On the M2 grid, Δx^+ is as low as 40 at the inter-element boundaries. It is, however, not entirely clear how the effective resolution of the Nek5000 grid should be defined. One could argue that the maximum spacing is the relevant measure. Regardless, if one were to decrease the grid size by a factor of 2 (which is desirable for better resolution of the outer scales), Δx^+ would start getting close to that of a wall-resolved simulation. This highlights the necessity of considering high Reynolds number flow for WMLES.

Table 1. Simulation parameters.

Parameter	Value
Inflow TBL thickness, δ_{99}^i	1 m
Freestream velocity, U_0	1 m/s
Kinematic viscosity, ν	$2.86 \cdot 10^{-5}$ m^2/s
Inflow Re-number, Re_θ	≈ 4060
Domain length	$150\,\mathrm{m} = 150\delta_{99}^i$
Domain height	$20\,\mathrm{m} = 20\delta_{99}^i$
Domain width	$20\,\mathrm{m} = 20\delta_{99}^i$
Time averaging length	$700\,\mathrm{s} = 700\delta_{99}^i/U_0$
Grid size, $y < 4\delta_{99}^i$	M1: $\approx 4 \cdot 10^6$, M2: $\approx 32 \cdot 10^6$

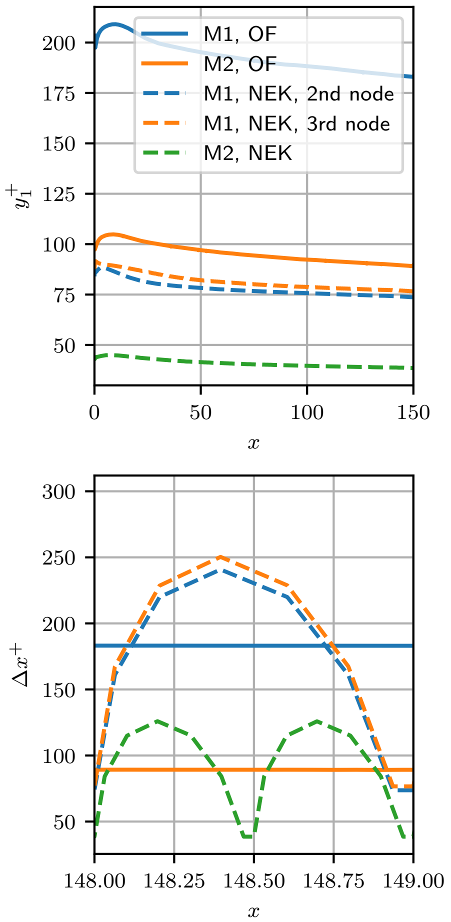

Figure 2. The size of the grid in wall units: y_1^+ (top) and Δx^+ (bottom). Note that $\Delta z^+ = \Delta x^+$.

WALL MODELLING

The role of the wall model is to provide the correct value of the wall shear stress τ_w for each boundary node. This task can be split in two: obtaining the sought value of τ_w and ingesting it into the simulation by means of a suitable boundary condition.

The general procedure for obtaining τ_w is to use a relationship coupling the stress with the LES solution at some point away from the wall. The distance to this point is an important parameter, which we will refer to as h. The simplest wall model can be constructed using the law of the wall, such as as Spalding's law (Spalding, 1961), which is used here. The law provides an algebraic expression connecting the streamwise velocity with the wall shear. Generally, this can be expressed as $F(u^+, y^+) = 0$. At each wall node, the value of u is then sampled at distance $y = h$, these values are inserted into F and the equation is solved for the friction velocity u_τ using Newton-Raphson iteration. The procedure is repeated at each time-step.

The value of τ_w is formed as a product of viscosity and the shear components of the rate of strain tensor evaluated at the boundary. Therefore, one can generally distinguish two main approaches to setting the obtained stress as a boundary condition. One is to use a Neumann boundary condition for the velocity field, effectively resulting in a slip velocity at the wall of such magnitude that the resulting rate of strain produces the desired value of τ_w. Alternatively, one can leave the no-slip condition for velocity intact and instead manipulate the viscosity at the wall in such a way that the when it multiplies the rate of strain, the necessary τ_w value is recovered.

In this work, we use the latter approach, which is now presented in more detail. Let ν_t be the value of SGS viscosity at the wall, and S_{ij} the components of the rate-of-strain tensor. Then, the magnitude of the wall shear stress is computed as

$$|\tau_w| = (\nu + \nu_t)\sqrt{S_{xy}^2 + S_{zy}^2} \tag{1}$$

It follows, that given $|\tau_w|$ from the wall model and the values of S_{ij} as computed at the wall, we can set ν_t according to

$$\nu_t = |\tau_w| / \sqrt{S_{xy}^2 + S_{zy}^2} - \nu \tag{2}$$

to prescribe $|\tau_w|$ at the boundary.

In OpenFOAM, this approach has been well tested in several works, e.g. Mukha *et al.* (2019). Conversely, in Nek5000 it has not been previously applied, and the comparative benefits with respect to the Neumann condition is a topic we are actively investigating, but will not focus on here. In the context of finite differences, the two approach have been analysed by Bae & Lozano-Durán (2021).

The import role of h in the accuracy of the predicted τ_w has been initially highlighted in Kawai & Larsson (2012) and later confirmed in other works, e.g. Rezaeiravesh *et al.* (2019); Frère *et al.* (2017). The consensus is that, independent of the underlying numerics, sampling from the first off-wall solution point leads to suboptimal results. More generally, sampling has to take place from a node where the velocity signal is accurate since any errors in u propagate directly into τ_w. In this context, it is observed that in the first off-wall node the error in u is always significant, see Kawai & Larsson (2012).

RESULTS

The figures in this section present results from 5 simulations. OpenFOAM simulations are denoted as OF in the legend, and Nek5000 simulations with NEK. For each code, a simulation on each of the meshes M1 and M2 is performed with h set to the 2nd and 3rd off-wall node, respectively. This corresponds to approximately the same distance from the wall (see Figure 5). Additionally, a Nek5000 simulation on the M1 grid with h set to the 3rd node is performed to highlight the importance of the selection of h.

To demonstrate the level of resolution of turbulent structures, Figure 5 shows a snapshot of the streamwise velocity taken at the outlet of the M2 grids. Qualitatively, the turbulence in the outer layer appears well-represented in both Nek5000 and OpenFOAM simulations. However, one should keep in mind that at the outlet the grid size is smallest relative to δ_{99}. Even so, the Nek5000 solution clearly exhibits numerical artefacts at element boundaries. Particularly the near-wall element is easily distinguished in the solution. This indicates that we can expect an improvement of the results using finer grids.

We begin the quantitative analysis of the results by looking at the performance of the wall modelling, which manifests itself in the values of the skin friction coefficient, c_f. The obtained values are shown in Figure 4. For reference, we use the wall-resolved LES (WRLES) data by Eitel-Amor *et al.* (2014), which, however, covers only a part of the Re_θ range of the WMLES. Therefore, the power law by Rezaeiravesh *et al.*

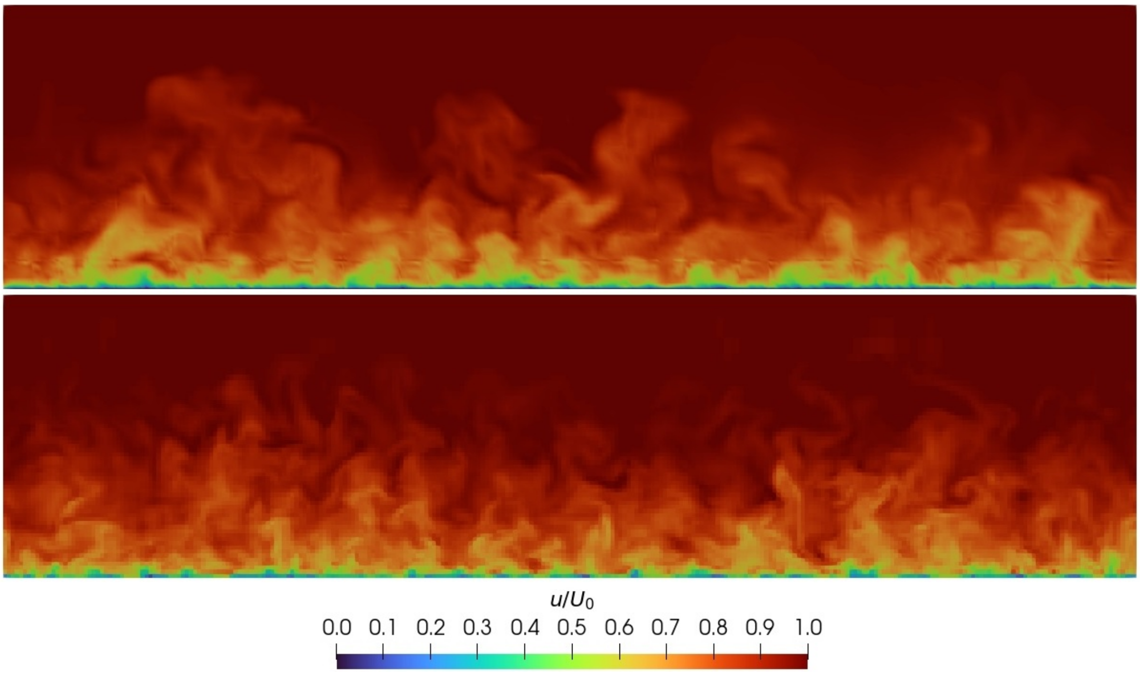

Figure 3. Streamwise velocity distribution at the outlet. Simulations on mesh M2, Nek5000 (top) and OpenFOAM (bottom)

(2016) is also depicted. The agreement between the WRLES and the power law is quite good.

The results from OpenFOAM simulations exhibit a significant over-prediction of c_f, although on the M2 grid the results are improved at high Re_θ. The accuracy is worse to what was previously reported at lower Re-number simulations in Mukha *et al.* (2021). There are methodological differences, which could explain that, particularly the fact that in Mukha *et al.* (2021) an unstructured grid adapted to the growth of the TBL was employed. The latter implies that the resolution of the TBL remains constant with x and that h is adapted to remain at the same fraction of the TBL thickness. It may therefore be possible to improve the OpenFOAM results, and further investigation is required.

The curves from Nek5000 simulations are more faithful to the reference power law. A very significant effect of h can be observed, however. The choice between 2nd or 3rd off-wall grid node on the M1 grid results in a shift of the c_f values, with significant under-prediction when the 2nd node is used. By contrast, the effect of grid resolution is more or less negligible per se—as long as an appropriate h is selected.

The profiles of the mean streamwise velocity are analysed next, see Figure 5. The location corresponds to $Re_\theta \approx 8183$. It is instructive to see whether the expected connection between the accuracy of c_f and the velocity prediction at the sampling point can be found. Indeed, we see that the OpenFOAM curves over-predict the reference profile, including the points corresponding to h. Looking at the Nek5000 profiles from grid M1 it is clear that the 3rd node is indeed in better agreement with the reference than the second, the latter lying below the curve. This is consistent with the c_f values. However, it is likely that the error in $\langle u \rangle$ is only part of the explanation for the c_f errors. For example, the Nek5000 simulation on the M2 grid also over-predicts the reference and the accuracy is only marginally better than that of the OpenFOAM value on the same grid. Yet the difference in c_f much larger. Finally, in inner scaling, the velocity values at the sampling points coincide perfectly with the reference log-law, as expected.

It is worth noting that the value of h has more or less no

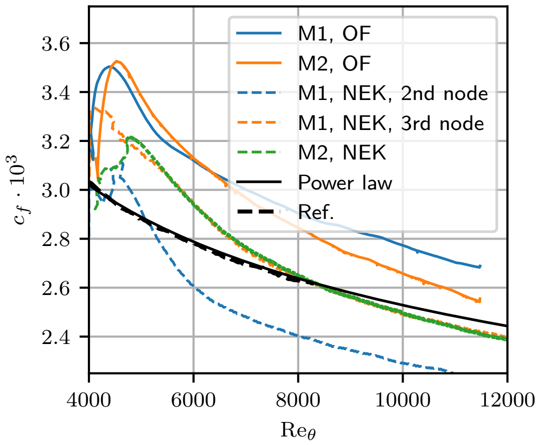

Figure 4. Development of the skin friction coefficient, c_f. Reference data from Eitel-Amor *et al.* (2014).

influence on $\langle u \rangle$, the Nek5000 profiles on the M1 grid overlap. So, the coupling between the sampled velocity and c_f is unidirectional. This has previously been observed in OpenFOAM, see Rezaeiravesh *et al.* (2019), however, one could expect a stronger coupling in Nek5000 since the velocity values are more strongly coupled via the underlying polynomial basis.

The accuracy of the Nek5000 solutions are clearly superior. However, the solution on the M2 mesh is worse than on M1 indicating that some fortuitous error cancellation may be at play. Interestingly, the plot in inner scaling shows no evidence of log-layer mismatch for the OpenFOAM solution, the discrepancy with the reference is instead further away from the wall.

Finally, we consider the second-order statistics, particularly the mean turbulent kinetic energy, $\langle k \rangle$ and the mean turbulent shear stress $\langle u'v' \rangle$. The profiles are shown in Figure 6. The accuracy of the OpenFOAM profiles is very similar to that reported in previous works, e.g. Mukha *et al.* (2019). The

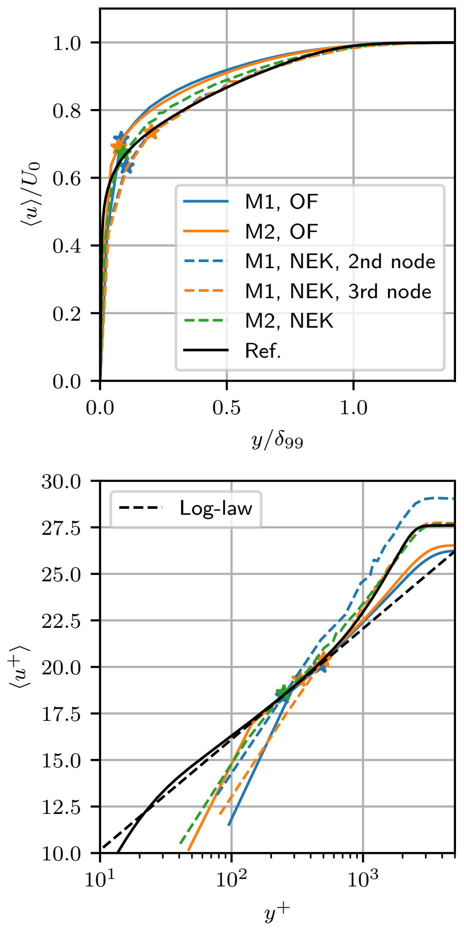

Figure 5. Mean velocity profiles at $Re_\theta \approx 8183$ in outer scaling (top) and inner scaling (bottom). Stars show the location of the sampling point. Reference data from Eitel-Amor *et al.* (2014). The log-law parameters are $\kappa = 0.387$ and $B = 4.21$ where selected according to Yamamoto & Tsuji (2018).

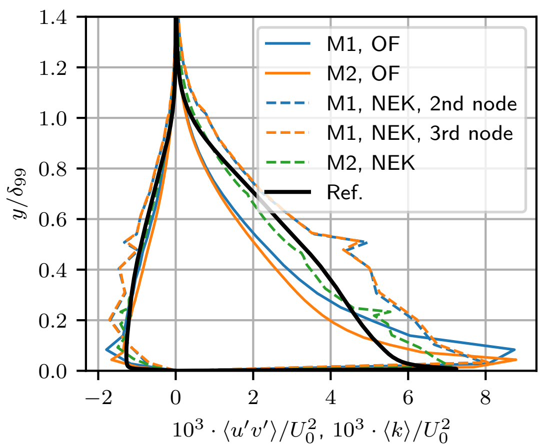

Figure 6. Profiles of the mean turbulent kinetic energy, $\langle k \rangle$, and the turbulent shear stress, $\langle u'v' \rangle$ at $Re_\theta \approx 8183$. Reference data from Eitel-Amor *et al.* (2014).

shear stress is well-predicted excluding small non-physical peak near the wall. For $\langle k \rangle$ one observes the typical pattern of over-prediction near the wall and then under-prediction closer to the free stream. In the Nek5000 solutions one clearly see the boundaries of the elements: they coincide with the spikes in $\langle k \rangle$. Clearly, on the M1 mesh the TBL is covered by 2 elements at the considered streamwise position. This resolution is too coarse to properly resolve the turbulent fluctuations and they are over-predicted. Note that even here the effect of h is negligible. On the M2 mesh the results are better and close in accuracy to that of OpenFOAM.

CONCLUSIONS

The most import outcome of this study is a successful WMLES of a spatially-evolving boundary layer in Nek5000. It is clear that, with a careful selection of simulation parameters, good agreement with reference data can be obtained. The simulations showed that the sampling height h should especially be chosen with care. The fact that Nek5000 outperforms OpenFOAM in terms of accuracy on equivalent grids is very encouraging. Using viscosity to enforce the wall shear stress appears to be a robust way to transmit the values predicted by the wall model into the simulation.

Several methodological question remain open: *i)* The necessary grid resolution to obtain convergence of statistics in the outer layer; *ii)* Length-scale computation for the subgrid viscosity, and selection of the model; *iii)* Selection of h, particularly its non-uniform distribution in space. All of these are currently the subject of our research.

For OpenFOAM, an important step is to try to apply the same unstructured meshing strategy as in (Mukha *et al.*, 2021) to see if that alleviates the issues with c_f predictions. Further, simulations on denser grids have to be performed to see if better agreement with the mean velocity profile can be obtained.

REFERENCES

Bae, H. J. & Lozano-Durán, A. 2021 Effect of wall boundary conditions on wall-modeled large-eddy simulation in a finite-difference framework. *Fluids* **6** (112).

Bose, S. T. & Park, G. I. 2018 Wall-modeled large-eddy simulation for complex turbulent flows. *Annual Review of Fluid Mechanics* **50**, 535–561.

Deville, E. H., Fischer, P. F. & Mund, E.H 2012 *High-Order Methods for Incompressible Flow*. Cambridge University Press.

Eitel-Amor, G., Örlü, R. & Schlatter, P. 2014 Simulation and validation of a spatially evolving turbulent boundary layer up to $Re_\theta = 8300$. *International Journal of Heat and Fluid Flow* **47**, 57–69.

Frère, A., de Wiart, C. C., Hillewaert, K., Chatelain, P. & Winckelmans, G. 2017 Application of wall-models to discontinuous Galerkin LES. *Physics of Fluids* **29**, 085111.

Hufnagel, L., Canton, J., Örlü, R., Marin, O., Merzari, E. & Schlatter, P. 2018 The three-dimensional structure of swirl-switching in bent pipe flow. *Journal of Fluid Mechanics* **835**, 86–101.

Jarrin, N., Benhamadouche, S., Laurence, D. & Prosser, R. 2006 A synthetic-eddy-method for generating inflow conditions for large-eddy simulations. *International Journal of Heat and Fluid Flow* **27** (4), 585–593.

Karniadakis, G. E., Israeli, M. & Orszag, S. A. 1991 High-order splitting methods for the incompressible Navier-

Stokes equations. *Journal of Computational Physics* **97** (2), 414–443.

Kawai, S. & Larsson, J. 2012 Wall-modeling in large eddy simulation: Length scales, grid resolution, and accuracy. *Physics of Fluids* **24** (1), 015105.

Larsson, J., Kawai, S., Bodart, J. & Bermejo-Moreno, I. 2016 Large eddy simulation with modeled wall-stress: Recent progress and future directions. *Mechanical Engineering Reviews* **3** (1), 1–23.

Mukha, T., Bensow, R.E. & Liefvendahl, M. 2021 Predictive accuracy of wall-modelled large-eddy simulation on unstructured grids. *Computers & Fluids* **221**, 104885.

Mukha, T., Rezaeiravesh, S. & Liefvendahl, M. 2019 A library for wall-modelled large-eddy simulation based on OpenFOAM technology. *Computer Physics Communications* **239**, 204–224.

Nicoud, F. & Ducros, F. 1999 Subgrid-scale stress modelling based on the square of the velocity gradient tensor. *Flow, Turbulence and Combustion* **62** (3), 183–200.

Poletto, R., Craft, T. & Revell, A. 2013 A new divergence free synthetic eddy method for the reproduction of inlet flow conditions for les. *Flow, Turbulence and Combustion* **91** (3), 519–539.

Rezaeiravesh, S., Liefvendahl, M. & Fureby, C. 2016 On grid resolution requirements for LES of wall-bounded flows. In *ECCOMAS Congress 2016*. Crete, Greece.

Rezaeiravesh, S., Mukha, T. & Liefvendahl, M. 2019 Systematic study of accuracy of wall-modeled large eddy simulation using uncertainty quantification techniques. *Computers and Fluids* **185**, 34–58.

Schlatter, P. & Örlü, R. 2010 Assessment of direct numerical simulation data of turbulent boundary layers. *Journal of Fluid Mechanics* **659**, 116–126.

Spalding, D. B. 1961 A single formula for the 'law of the wall'. *Journal of Applied Mechanics* **28** (3), 455–458.

Vreman, A. W. 2004 An eddy-viscosity subgrid-scale model for turbulent shear flow: Algebraic theory and applications. *Physics of Fluids* **16** (10), 3670–3681.

Yamamoto, Y. & Tsuji, Y. 2018 Numerical evidence of logarithmic regions in channel flow at $Re_\tau = 8000$. *Physical Review Fluids* **3** (1), 012602.